

Evaporation Rate Measurement of Water and Liquid 1-Alkanols across Air–Liquid Interface Using Thermogravimetry

Muhammad Rusdi and Yoshikiyo Moroi*

Chemistry and Physics of Condensed Matter, Graduate School of Sciences, Kyushu University-Ropponmatsu, Fukuoka 810-8560

(Received August 14, 2002)

Evaporation rate measurements of water across air/water interface were made by using a thermogravimetry technique. A sample liquid was held in a partially filled, open-topped pan in a furnace tube, through which dry air was flowing. The effect of the flow rate of the dry air on the evaporation rate was very large at lower flow rates, while it became smaller at higher flow rates. The evaporation rate of water over the temperature range 298.2–333.2 K was studied in order to obtain the activation energy for the evaporation. The energy was found to decrease with increasing temperature. A newly developed equation was used to analyze the evaporation rate. Purified liquid 1-alkanols (carbon number = 4, 6, 8, 10, and 12) were employed as test substances in order to estimate the effects of terminal $-CH_2OH$ group and of residual CH_2 groups on the activation energy. The contribution of $-CH_2OH$ group to the activation energy was found to slightly decrease with increasing temperature, while the contribution of residual CH_2 group increased with increasing chain length; the temperature-dependence remained almost the same irrespective of the alkyl chain.

Material transport across an interface or a membrane is important not only for dynamic aspects of surface chemistry but also for living tissues. Evaporation is a typical example of material transport across air/liquid interface. Evaporation of liquids and condensation of vapors are quite often met for innumerable processes of everyday life. Their applications are very familiar; the list grows longer if the topic is broadened to include such related phenomena as evaporation cooling.[1,2]

The studies on evaporation rate across air/liquid interface have covered three areas: (i) the evaporation rate of liquid materials across air/liquid interfaces; (ii) the evaporation rate of water across air/aqueous solution interfaces; and (iii) the evaporation rate of water across air/solution interfaces covered by an insoluble monolayer. The third type was summarized in a review article by Barnes in 1986.[3] Concerning the evaporation rate of liquid materials across air/liquid interfaces, only a few papers have appeared.[4–7] In the present study, an investigation of type (i) was made in order to see whether our evaporation model is reasonable or not from the kinetics point of view and also to investigate the contributions of $-CH_2OH$ group and of residual CH_2 group to the total activation energy of liquid 1-alkanols. For the above purposes, the evaporation rate measurement for water becomes quite an important index. Even though no concentration gradient is generated within the liquid for the case of evaporation of a pure liquid,[8] the concentration gradient of the vapor phase becomes a driving force in the evaporation process.

Experimental

Materials. 1-Alkanols (carbon number = 4, 6, 8, 10, and 12) were purchased from G.L. Sciences. The purity of each 1-alkanol was above 99%, and they were used as received. The reported melting and boiling points of 1-alkanols are shown in Table 1, which is just to assist a reader to recall their basic properties. The water used was distilled twice from alkaline permanganate solution.

Method. The apparatus was based upon a conventional thermogravitational analysis (Fig. 1, Rigaku Thermo Plus 2); the area

Table 1. Melting and Boiling Points of 1-Alkanols[9]

1-Alkanol	Melting Point/°C	Boiling Point/°C
Butanol	−89.8	117.7
Hexanol	−44.6	157.6
Octanol	−15.5	195.1
Decanol	6.9	231.1
Dodecanol	24.0	259.0

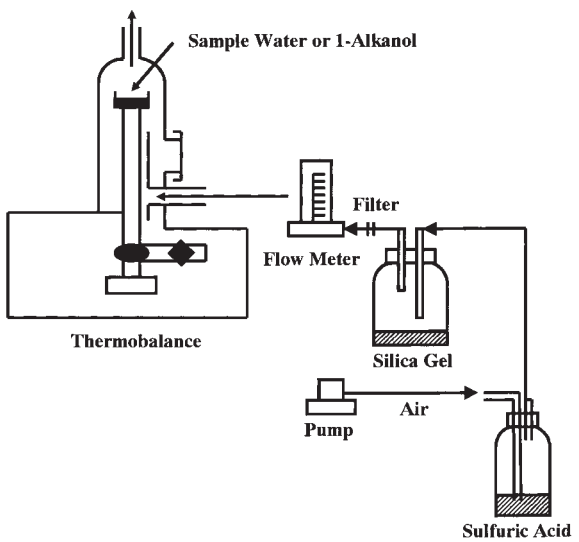

Fig. 1. Schematic illustration of modified apparatus for thermogravimetry.

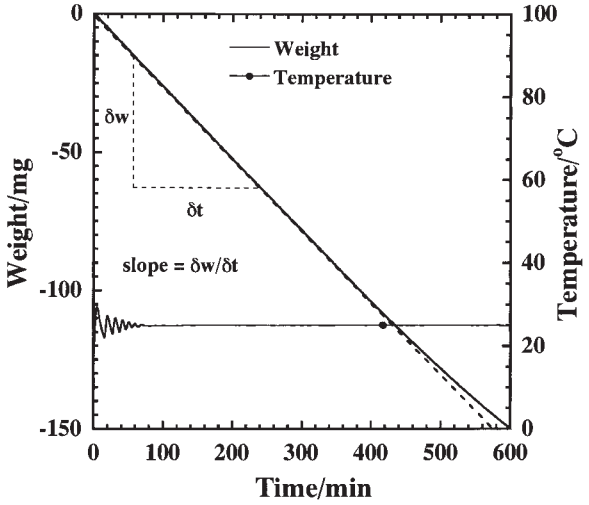

Fig. 2. Raw data for change of weight and temperature (solid line: experimental change, broken line: straight line fit).

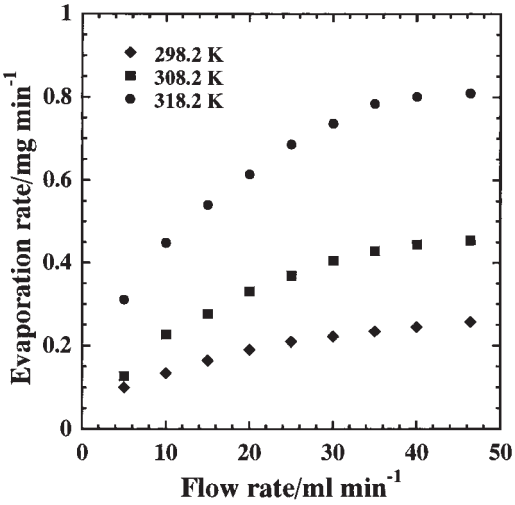

Fig. 3. Dependence of evaporation rate by weight of water on flow rate of dry air.

of a platinum sample pan was large, 0.739 cm^2, to make edge effects as small as possible. A constant volume (150 μL) of liquid sample was poured into the shallow platinum pan and set for the gravitational measurement, where the height from liquid level to mouth of the pan was 0.478 cm. The apparatus can detect the changes of both weight and temperature with time, simultaneously; the temperature was controlled within ±0.1 °C throughout the run, except for initial fluctuations for 55 min at 25 °C (Fig. 2). Temperature of the sample pan was monitored by a thermister just below the pan. The initial depth of liquid is 0.20 cm; therefore, such a thin layer of liquid is easy for the thermister to follow. Moisture in the flow air was completely removed by passing it through concentrated sulfuric acid firstly and by keeping it over dried silica gel secondly. Then, the dry air passed two times through a filter of pore size 0.22 μm (Millipore, SLGV025LS) in order to remove dust; the flow rate was controlled by a flow meter with a needle bulb.[10] The experimental reproducibility was such that the weight decrease with time for each run could trace one line for the same sample (Fig. 2).

Results and Discussion

In general, the evaporation rate can be controlled by any of the following three possible processes. Firstly, molecular diffusion across a stagnant vapor layer just above a liquid may be rate-determining in one experimental geometry. Secondly, there may be a significant energy barrier to the evaporation process for molecules leaving a vapor/liquid interface. Thirdly, evaporation of a volatile species from a multi-component liquid mixture may generate concentration gradients within the liquid, and therefore, the gradient may be rate-determining for mass transfer within the liquid.[8]

The evaporation rate of liquid in the unit of mol s^{-1} cm^{-2} naturally depends on the shape of the cell used and on experimental conditions. For example, if the distance from the liquid level to the mouth of the cell is longer, the rate will become slower. However, the rate is not always inversely proportional to the distance but depends on the area of the cell and on the flow rate of gas passing around the cell. When the area is large and the flow rate is fast even for the same distance, the flowing gas easily comes into the inner space of the cell and agitates the stagnant vapor just above the liquid, which leads to faster evaporation rate. In other words, several factors do affect the evaporation rate of liquids, although the concentration gradient of evaporating molecules is quite important. The important point is, however, to keep the factors constant. In that case, these factors would disappear when the logarithm of the evaporation rate is differentiated with respect to temperature, and only the temperature-dependent factors affecting the evaporation rate would remain for evaluation of the activation energy of liquid evaporation.

The material flow rate (J) at gas/liquid interface is definitely determined by the concentration profile of the material in the interfacial region. Namely, this is given by the Fick's first law:[11]

$$J = -D^{\mathrm{l}}\left(\frac{\partial c^{\mathrm{l}}}{\partial x}\right)_{x=0} = -D^{\mathrm{g}}\left(\frac{\partial c^{\mathrm{g}}}{\partial x}\right)_{x=0} \quad (1)$$

where D^{l} and D^{g} are the diffusion coefficient of material in a liquid phase and a gas phase, respectively, and Eq. 1 represents continuity of material flow. As for a gaseous phase, temperature dependence of the diffusion coefficient is important, because molecular flux J in a gaseous phase is controlled by Eq. 1. Therefore, the temperature dependence of logarithms of D^{g} and the concentration gradient (or density gradient) comes to relate with the activation energy of material flow at a gas/liquid interface. The concentration gradient term depends on experimental conditions, which strongly suggests that the terms that can be kept constant should not be varied throughout the experiment. In the present study, the flow rate (J) is equal to the evaporation rate (k).

Water Evaporation. We first consider the rate of weight decrease of water by vaporization from a liquid water surface, upon which there is no external resistance or barrier to the water evaporation. The evaporation rate of water is proportional to the area of the liquid surface and, at the same time, to the difference in partial vapor pressure between just above the liquid surface and in the surroundings. Narusawa and Springer measured evaporation rate of water at several pres-

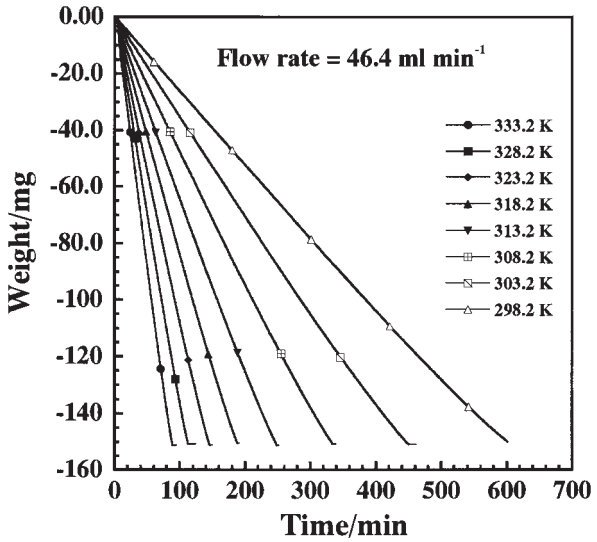

Fig. 4. Weight decrease of water with time at different temperatures from 298.2 to 333.2 K.

sure differences $\Delta P = P^{sat} - P$, where P^{sat} was equilibrium saturation vapor pressure corresponding to the surface temperature and P was vapor pressure in the surroundings. They found that mass transfer rate was faster at larger pressure differences.[12]

The evaporation rate must be affected by vapor pressure above a liquid surface. We therefore investigated first the effect of flow rate of dry air on water evaporation rate by weight at three different temperatures: 298.2, 308.2, and 318.2 K. As shown in Fig. 3, an effect of the flow rate is very significant at lower flow rate, while it becomes smaller at higher flow rate. In the present experiment, therefore, the flow rate was kept constant at 46.4 mL min^{-1} in order to minimize the effect of the flow rate drift, where the evaporation rate becomes almost constant irrespective of the flow rate and of temperature. The vapor of a liquid just above the surface forms a stagnant vapor layer which influences the evaporation rate of liquid.[12] Using the maximum flow rate, the stagnant layer could be reduced as much as possible for the present pan under the present experimental conditions. In addition, the thickness of the layer remains almost constant, as is mentioned later.

An evaporation rate equation in terms of thick stagnant layer, gas flow rate, vapor diffusion coefficient, and some geometrical parameters was derived by Fletcher et al.[13] Unfortunately, their theory could not apply to the analysis of our experimental data, partly because inner height and radius of our shallow sample pan are 0.681 cm and 0.485 cm, respectively, and partly because our flow rate of dry air could partially agitate an inner space of the pan. According to their theory, the evaporation rate should decrease by 1.4-fold by increasing the stagnant layer h by 1.4-fold. In reality, however, the rate decreased by just 1.1-fold.

Evaporation rate of water works as an important reference for further study on water evaporation of the types (ii) and (iii) mentioned above. The time dependence of weight decrease was done over the temperature range 298.2–333.2 K. As shown in Fig. 4, the slope of decrease became significantly different, depending on temperature.

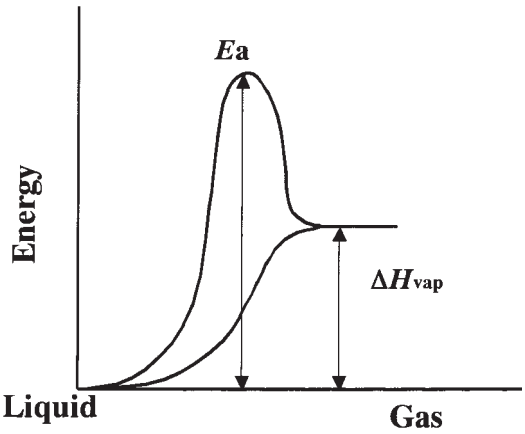

Fig. 5. Schematic diagram showing energy transitions from liquid to vapor.

Table 2. Evaporation Rate (k) of Water

T/K	k/mol s^{-1} cm^{-2}	ln $k(y)$[a)]
298.2	3.26×10^{-7}	−14.9
303.2	4.25×10^{-7}	−14.7
308.2	5.70×10^{-7}	−14.4
313.2	7.71×10^{-7}	−14.1
318.2	1.01×10^{-6}	−13.8
323.2	1.32×10^{-6}	−13.5
328.2	1.70×10^{-6}	−13.3
333.2	2.18×10^{-6}	−13.0

a) y is ordinate value in Fig. 6.

The evaporation process is endothermic; the schematic diagram is shown in Fig. 5.[14] The energy transition on going through the kinetic pathway involves an activation energy E_a as noted in the diagram. The activation energy is a minimum energy needed for the process to go on. On the other hand, the enthalpy change of evaporation (ΔH_{vap}) is concerned only with the energy difference between the initial (liquid) and the final (vapor) states, and is independent of the pathway. ΔH_{vap} corresponds to the minimum energy that must be supplied to the system in order to convert a unit amount of substance from liquid to vapor under the condition of phase equilibrium. Thus, E_a is larger than ΔH_{vap}. This is an important point of liquid evaporation, as is mentioned later.

Activation energy of water evaporation can be calculated from temperature dependence of the evaporation rate or the initial linear slope of Fig. 4 by employing the Arrhenius equation:

$$k = Ae^{-E_a/RT} \tag{2}$$

where k is the evaporation rate per unit area (mol s^{-1} cm^{-2}) and E_a is the activation energy. Thus, temperature dependence of evaporation rate is required for an evaluation of E_a. The above equation applies regardless of whether the Arrhenius plot is linear or not; if it is not, the activation energy changes with temperature.

In order to calculate the activation energy of water evaporation, some parameters are needed; they are listed in Table 2 and plotted in Fig. 6. The activation energy varies with the

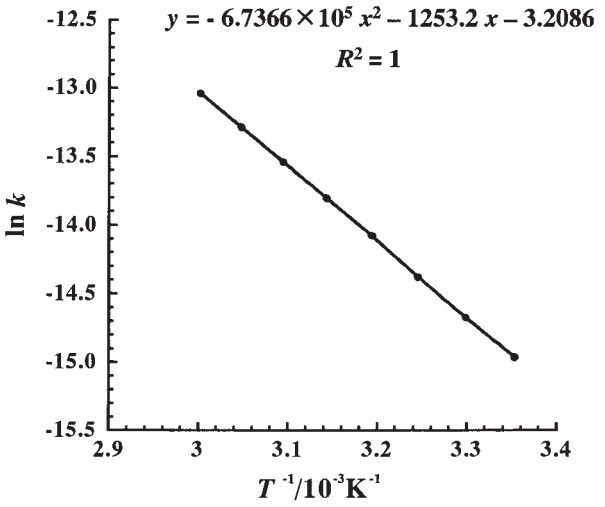

Fig. 6. Plots of $\ln k$ vs T^{-1} for liquid water: $y = \ln k$ and $x = T^{-1}$.

Table 3. Activation Energy (E_a) and Enthalpy Change (ΔH_{vap}) of Evaporation for Liquid Water

T/K	E_a/kJ mol^{-1}	E_a[a)]/kJ mol^{-1}	ΔH_{vap}[b)]/kJ mol^{-1}
298.2	48.0	45.3	44.0
303.2	47.4	45.1	43.9
308.2	46.8	44.9	43.6
313.2	46.2	44.7	43.4
318.2	45.6	44.5	43.2
323.2	45.1	44.4	43.1
328.2	44.6	44.3	43.0
333.2	44.1	44.1	42.7

a) $\Delta H_{vap} + RT/2$. b) Estimated from temperature dependence of vapor pressure.

temperature (Table 3, column 2), because the Arrhenius plot is not linear. These values decreased quite slowly with increasing temperature over the whole temperature range: 298–333 K. This is because intermolecular interaction between water molecules is mainly due to the particular donor-acceptor hydrogen bonding mechanism which is only slightly dependent on temperature in the liquid state.

On the other hand, the maximum evaporation rate (k) of water per unit area can be also estimated from the Hertz–Knudsen equation[15,16]

$$k = \left(\frac{RT}{2\pi M}\right)^{1/2} p^{sat} \tag{3}$$

where R is the gas constant, T is absolute temperature, M is a molecular mass, and P^{sat} is saturation pressure. This equation predicts an absolute upper limit on the rate at which molecules can escape from liquid interface into a perfect vacuum. In fact, the evaporation rate calculated by Eq. 3 is 1.7×10^5 times faster than the experimental rates. In this sense, the Hertz–Knudsen equation is not applicable to the rate analysis for usual evaporation data.

Based on the kinetic theory of diffusion,[17] the self-diffusion coefficient D^g of gas molecules is given by

$$D^g = \frac{1}{3}\lambda\bar{c} \tag{4}$$

where λ is the mean free path of molecules ($1/(\sqrt{2}\pi Nd^2)$) and $\bar{c}$ is the average speed of molecules ($\sqrt{8RT/\pi M}$). Then, D^g is given by the following equation:

$$D^g = \frac{2}{3\pi^{3/2}N}\sqrt{\frac{RT}{Md^4}} \tag{5}$$

where N is the number of molecules per unit volume, d is a molecular diameter, and R, T, and M are the same as above. Numerical values of D^g are available from a reference book; $D^{g,r} = 0.242$ cm^2 s^{-1} at 293 K and 0.399 cm^2 s^{-1} at 373 K for gaseous water molecules.[9] When the D^g values calculated by Eq. 5 are compared with the above values, the ratio ($D^g/D^{g,r}$) becomes 0.984 and 0.860 at 298 and 373 K, respectively, where the following values are used: $d = 2.72 \times 10^{-8}$ cm, $N = 2.469 \times 10^{19}$ and 1.969×10^{19} molecules cm^{-3} at 298 and 373 K, respectively. Now it becomes clear that Eq. 5 can not be applied to evaporation rate as it stands, although it is reasonable. However, it is quite possible to rewrite Eq. 5 as $D^g = K\alpha(T)\sqrt{T}$. The point of Eq. 1 is the concentration gradient. Generally, it is roughly expressed by an average concentration gradient at a stationary state as

$$\frac{dc}{dx} = \frac{c - c^{eq}}{l} \tag{6}$$

where c^{eq} is concentration derived from the saturation equilibrium vapor pressure (P^{eq}) and c is the concentration at a distance l from the surface. In our present case, c is assumed to be negligibly small compared with c^{eq} at the place where the diffusion starts. Combining Eqs. 1, 5, and 6, the evaporation rate then becomes the following equation:

$$k = K\alpha(T)\sqrt{T}\frac{P^{eq}}{l} \tag{7}$$

with

$$K = 2R^{1/2}/(3\pi^{3/2}M^{1/2}) \tag{8}$$

$$\alpha(T) = \frac{1}{Nd^2} \tag{9}$$

where K is a constant irrespective of experimental conditions as is clear from the above equation, while the rest of the right hand side of Eq. 7 depends on experimental conditions. The l value obtained from the reference $D^{g,r}$ value and from the evaporation rate becomes 0.99 cm at 298 K, which is quite reasonable judging from our evaporation pan. If the logarithm of Eq. 7 is differentiated with respect to inverse temperature, one obtains the following relation:

$$\frac{d\ln k}{d(1/T)} = \frac{d\ln P^{eq}}{d(1/T)} + \frac{1}{2}\frac{d\ln T}{d(1/T)} + \frac{d\ln\dfrac{\alpha(T)}{l}}{d(1/T)} \tag{10}$$

Substitutions of Eq. 2 and the Clausius-Clapeyron equation into Eq. 10 yield:

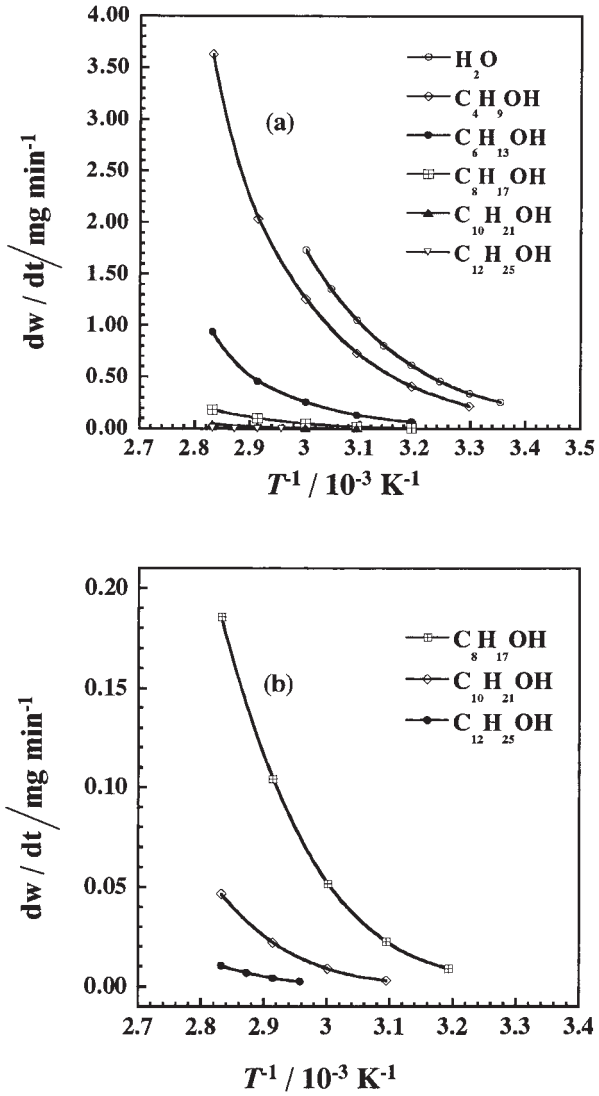

Fig. 7. (a) Changes of evaporation rate with temperature for water and 1-alkanols. (b) Changes in expanded scale of the ordinate for 1-alkanols whose carbon number is 8, 10, and 12.

$$E_a = \Delta H_{vap} + \frac{RT}{2} - R\left\{\frac{d\ln\beta(T)}{d(1/T)}\right\} \tag{11}$$

with

$$\beta(T) = \frac{1}{Nd^2l} \tag{12}$$

where E_a is the activation energy, ΔH_{vap} is the enthalpy change of evaporation, and $\beta(T)$ is a function of temperature. Therefore, if β is assumed constant, the E_a value is always greater than the ΔH_{vap} value by $RT/2$, 1.23 kJ mol^{-1} at 298.2 K (Table 3, column 3). This is the case of our results at higher temperatures, although the difference between them becomes larger than $RT/2$ at lower temperatures. This is due to the presence of the last term in Eq. 11. In addition, apparent values of evaporation coefficient (ratio of an evaporation rate to the rate by Eq. 3) were less than unity for many experimental data, which were summarized by Marek and Straub.[18] If one judges from the values in Table 3, our experimental data are quite reasonable. In addition, almost all of the activation energy is found to be used to break the hydrogen bonds in order for water molecules to escape from the liquid phase to the vapor phase.

Finally, the stagnant layer needs some explanation. When the flowing air is assumed to be saturated with the vapor having a vapor pressure of water at a definite temperature, the evaporation rate (k_{sat}) is determined by the flow rate. Therefore, the value of $k/(k_{sat}\sqrt{T})$ becomes an index of $K\alpha(T)/l$ of Eq. 7. The values obtained from the maximum evaporation rates in Fig. 3 are 1.39×10^{-2}, 1.39×10^{-2}, and 1.48×10^{-2} K$^{-1/2}$ at 298.2, 303.2, and 313.2 K, respectively. These values strongly suggest a stagnant layer of almost constant thickness at different temperatures under the present experimental conditions.

Evaporation of 1-Alkanols from the Liquids. 1-Alkanols with the carbon numbers of 4, 6, 8, 10, and 12 were also examined in this research. Ethanol (bp: 351 K) was investigated, but the liquid had totally evaporated before the measurement temperature became stabilized. The dependences of evaporation rate on temperature are illustrated in Fig. 7, from which the evaporation rate for 1-alkanols is found to be strongly temperature-dependent. As was done for liquid water, fitting of the evaporation rates to a quadratic-equation curve was made in order to calculate the activation energy at different temperatures, because the rate change did not give an absolutely straight line (see Fig. 8, which is similar to Fig. 6).

The activation energies of 1-alkanols are listed in Table 4. As shown in Table 4, the activation energy of the evaporation increases as the chain length becomes longer. On the other hand, the activation energy decreases with increasing temperature.

The relationship between vapor pressure and temperature can be derived from fundamental thermodynamics. The Clausius–Clapeyron equation is an exact thermodynamic relationship and therefore provides an important connection among properties of different phases. When applied to the calculation of latent heat of vaporization, its use presupposes knowledge of a vapor pressure vs temperature relation. Such relations are empirical. Thermodynamics imposes no model of material behavior, either in general or for particular substances. The Antoine equation, which is satisfactory and widely used, has the following form[19]

$$\ln P = A - \frac{B}{T + C} \tag{13}$$

where P is vapor pressure in mmHg, T is temperature in Kelvin, and A, B, and C are the Antoine constants for given temperature range recorded in the book by Stephenson and Malamowski.[20] The enthalpy change of vaporization (ΔH_{vap}) can then be evaluated for an ideal gas by the Clausius–Clapeyron equation:

$$\Delta H_{vap} = \frac{RBT^2}{(T + C)^2} \tag{14}$$

where R is the molar gas constant.

The Antoine constants[20] for 1-alkanols are listed in Table 5. Using Eq. 14, one can calculate ΔH_{vap} of 1-alkanols as shown in Table 6, in which ΔH_{vap} values for $C_{12}H_{25}OH$ are evaluated

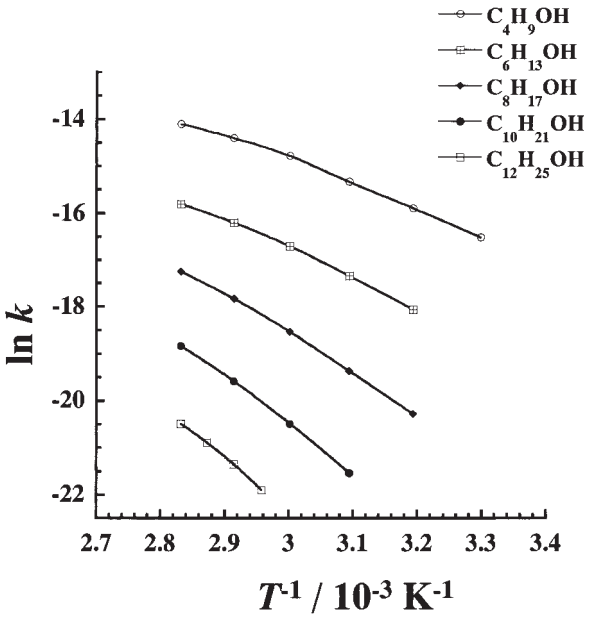

Fig. 8. Plots of $\ln k$ vs T^{-1} for liquid 1-alkanols.

Table 4. Activation Energy (kJ mol^{-1}) of Evaporation for 1-Alkanols

T/K	C_4H_9OH	$C_6H_{13}OH$	$C_8H_{17}OH$	$C_{10}H_{21}OH$	$C_{12}H_{25}OH$
303.2	57.9	—	—	—	—
313.2	55.9	68.8	80.9	—	—
323.2	54.0	65.5	77.8	91.0	—
333.2	52.2	62.5	74.9	87.5	—
338.2	—	—	—	—	99.9
343.2	50.5	59.6	72.2	84.5	96.7
348.2	—	—	—	—	93.4
353.2	48.9	56.8	69.7	81.2	90.6

Table 5. The Antoine Constants of 1-Alkanols

1-Alkanol	A	B	C	Temperature/K
C_4H_9OH	6.5417	1336.0	−96.348	323–413
$C_6H_{13}OH$	6.4127	1422.0	−107.71	325–431
$C_8H_{17}OH$	6.3941	1540.6	−115.62	328–400
$C_{10}H_{21}OH$	6.5740	1761.7	−113.99	349–410
$C_{12}H_{25}OH$	8.1111	3297.4	0	288–333

Table 6. Values of ΔH_{vap} (kJ mol^{-1}) at Several Temperatures

T/K	C_4H_9OH	$C_6H_{13}OH$	$C_8H_{17}OH$	$C_{10}H_{21}OH$	$C_{12}H_{25}OH$[a)]
323.2	51.9	61.2	71.5	80.5	—
333.2	50.6	59.4	69.2	77.9	—
338.2	—	—	—	—	95.2
343.2	49.4	57.8	67.1	75.6	93.3
348.2	—	—	—	—	91.1
353.2	48.4	56.4	65.2	73.6	89.0

a) From temperature dependence of vapor pressure.[21]

from temperature dependence of the vapor pressure, because the value of the parameter C is zero (Table 5). Figure 5 shows that E_a is larger than ΔH_{vap}. From the calculations above (Tables 4 and 6), one sees that the heats of vaporization for

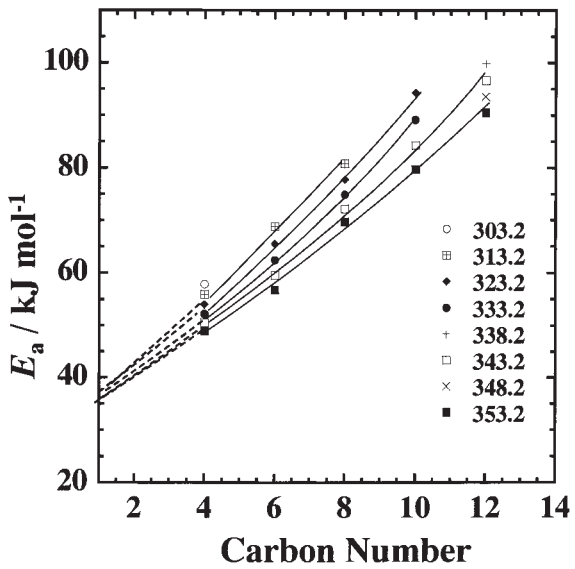

Fig. 9. The activation energy of evaporation vs carbon number of 1-alkanols at different temperatures.

Table 7. Quadratic-Equation or Curve Fitting for Activation Energy of Evaporation for 1-Alkanols: $x = C_n - 1$, Where C_n is the Number of Carbon Atoms of 1-Alkanols

T/K	The equation	R^2
313.2	$y = 0.02x^2 + 6.045x + 37.575$	1
323.2	$y = 0.0994x^2 + 4.97x + 38.183$	1
333.2	$y = 0.1406x^2 + 4.24x + 38.062$	0.9997
343.2	$y = 0.1121x^2 + 4.274x + 36.356$	0.9989
353.2	$y = 0.0946x^2 + 4.166x + 35.015$	0.9975

1-alkanols are smaller than the activation energies and, at the same time, the heats increase as alkyl chains of the alcohols become longer. The same temperature dependence is also observed for the activation energy, which means that the activation energy for 1-alkanols is closely related with the heat of vaporization. However, the increasing difference between them results from increased temperature-dependence of the parameter β with alkyl chain, which can be expected from the increased complexity of molecular structure with increasing alkyl chain. An abrupt jump in ΔH_{vap} value for $C_{12}H_{25}OH$ is due to a different cause.

The surface tension of a liquid is an index of molecular interaction at vapor/liquid interface. The surface tension of the present alcohols decreases with increasing temperature, an 18.2% decrease at maximum from 303.2 to 353.3 K,[22] which strongly indicates decreasing molecular interaction with rising temperature. The molecular interaction should be closely related with the activation energy of the liquid vaporization, which was verified by the decreasing activation energies with increasing temperature (Table 4), although the temperature dependence of the activation energy resulted from several factors other than surface tension.

Dependence of the activation energy on the carbon number of 1-alkanols is illustrated in Fig. 9. The results in Fig. 9 show that the activation energy of 1-alkanols was found to decrease with increasing temperature. In addition, temperature depen-

Table 8. Contribution of a Terminal $-CH_2OH$ and Residual CH_2 Groups to E_a ($kJ\,mol^{-1}$) for Evaporation of 1-Alkanols

T/K	$-CH_2OH$	$C_n = 4$ ($x = 3$)		$C_n = 6$ ($x = 5$)		$C_n = 8$ ($x = 7$)		$C_n = 10$ ($x = 9$)		$C_n = 12$ ($x = 11$)	
		$3(-CH_2-)$	$-CH_2-$	$5(-CH_2-)$	$-CH_2-$	$7(-CH_2-)$	$-CH_2-$	$9(-CH_2-)$	$-CH_2-$	$11(-CH_2-)$	$-CH_2-$
313.2	37.58	18.49	6.17	31.23	6.25	44.28	6.33	—	—	—	—
323.2	38.18	16.76	5.57	29.82	5.96	44.53	6.36	60.83	6.76	—	—
333.2	38.06	15.25	5.08	28.23	5.65	43.45	6.21	60.93	6.77	—	—
343.2	36.36	14.84	4.95	26.98	5.40	40.90	5.84	56.62	6.29	74.14	6.74
353.2	35.02	14.20	4.73	25.56	5.11	36.68	5.24	50.22	5.58	65.12	5.92

dence of the activation energy is slightly larger for longer alkyl chains than for shorter ones. It means that, when temperature decreased, 1-alkanol molecules need more extra energy to escape from the liquid to gaseous phase for longer alkyl chains. In addition, evaporation rate was influenced by hydrophobic interactions, which is nearly proportional to alkyl chain length of 1-alkanols. Xia and Landman investigated evaporation and condensation of liquid n-C_6H_{14} and n-$C_{16}H_{34}$ by molecular dynamics simulation. The result showed that for n-$C_{16}H_{34}$ in the vapor the *trans* (t) and *gauche* (g_+, g^-) conformations are distributed almost equally [i.e., $(t, g_+, g^-) = (33, 31, 36)$], while in the hot liquid the fraction of the *trans* conformations is much larger [i.e., $(t, g_+, g^-) = (66, 17, 17)$]. For n-C_6H_{14}, on the other hand, a reverse trend was found with the fraction of *trans* conformations larger in the vapor [i.e., $(t, g_+, g^-) = (83, 10, 7)$] than in the hot liquid [i.e., $(t, g_+, g^-) = (72, 14, 14)$].[23] The point of the above is that the *trans* conformation is predominant for both liquids. In the present case, too, the molecules seem mostly elongated by the *trans* conformation (Fig. 9).

Finally, the contribution of a terminal $-CH_2OH$ group and of residual CH_2 group to the total activation energy of evaporation for 1-alkanols whose carbon number is 4, 6, 8, 10, and 12 was interpreted by a quadratic equation or a quadratic curve fitting. The equations are listed in Table 7 at temperatures from 313.2 to 353.2 K. Extrapolating the y value to the carbon number one obeying the quadratic curve fitting, one finds that the values become nearly equal to the estimated value ($38.9\ kJ\,mol^{-1}$) of activation energy of methanol at 333.2 K, where the β value in Eq. 10 is assumed constant. In other words, the contribution of $-CH_2OH$ group to the total activation energy could be obtained as the extrapolated value at the carbon number one. According to the constant values in Table 7, the contribution of $-CH_2OH$ group to the activation energy becomes smaller with increasing temperature. This extrapolated value (E_a of $-CH_2OH$) is $37.04 \pm 1.20\ kJ\,mol^{-1}$ over the temperature range from 313.2 to 353.2 K. This fact seems reasonable, because the estimated ΔH_{vap} values for methanol from the vapor pressure change from 37.0 to 38.0 $kJ\,mol^{-1}$ over the temperature range 313.2–353.2 K. Beside that, interaction between 1-alkanol molecules is partially due to hydrogen bonding, say less than 50% of the total activation energy, judging from the values for two hydrogen bonds of water in Table 3, and is partially due to a dispersion force which is temperature-dependent. In addition, the effect of the hydrogen bonding became less for longer alkyl chains.

The residual energy value can be attributed to methylene groups. The values thus obtained are listed in Table 8. The contribution of methylene groups became larger for longer alkanols, while the contribution of $-CH_2OH$ group was larger for shorter alkanols. This might be caused by the fact that the terminal –OH group still has a strong influence on the dispersion interaction among alkyl chains for shorter chain alkanols. At the same time, the temperature-dependence of the CH_2 contribution was slightly larger with increasing alkyl chain length. This is because attractive interaction among alkyl chains comes to play a more important role than hydrogen bonds between hydroxy groups with increasing alkyl chains.

The conclusions pertaining to the present evaporation rates of water and liquid 1-alkanols across air/liquid interface can be summarized as follows:

1. The effect of flow rate of dry air on evaporation rate was very significant at lower flow rate, while it became smaller at higher flow rate.
2. The activation energy of water evaporation was found to be $48.0\ kJ\,mol^{-1}$ at 298.2 K, which is higher than the enthalpy change of evaporation, $44.0\ kJ\,mol^{-1}$.
3. The activation energy of evaporation for 1-alkanols whose carbon number was 4, 6, 8, 10, and 12 decreased with increasing temperature, while the energy increased with increasing alkyl chain length.
4. The contribution of a terminal $-CH_2OH$ group to the activation energy slightly decreased with increasing temperature. On the contrary, that of residual CH_2 groups decreased more steeply with increasing temperature, where the contribution increased with increasing chain length.

This work was supported by Grant-in-Aid for Scientific Research No. 10554040 from the Ministry of Education, Science and Culture, Japan and a grant from The Cosmetology Research Foundation, which are gratefully acknowledged.

References

1 V. K. La Mer, "Retardation of Evaporation by Monolayer," Academic Press, New York (1962).
2 F. E. Jones, "Evaporation of water, with emphasis on applications and measurements," Lewis Publishers, Michigan (1992).
3 G. T. Barnes, *Adv. Colloid Interface Sci.*, **25**, 89 (1986).
4 S. P. Lin and M. J. Hudman, *J. Thermophys. Heat Transfer*, **10**, 497 (1996).
5 K. D. Ohare and P. L. Spedding, *Chem. Eng. J. and The Biochem. Eng. J.*, **48**, 1 (1992).
6 J. H. Clint, P. D. I. Fletcher, and I. T. Todorov, *Phys. Chem. Chem. Phys.*, **1**, 5005 (1999).
7 K. Lunkenheimer and M. Zembara, *J. Colloid Interface Sci.*, **188**, 363 (1997).
8 K. J. Beverley, J. H. Clint, and P. D. I. Fletcher, *Phys.*

Chem. Chem. Phys., **2**, 4173 (2000).
9 R. L. David (editor-in-chief), ''Handbook of Chemistry and Physics,'' 82nd ed, CRC Press, New York (2001).
10 Y. Moroi, T. Yamabe, O. Shibata, and Y. Abe, *Langmuir*, **16**, 9697 (2000).
11 P. C. Hiemenz, ''Principles of Colloid and Surface Chemistry,'' Marcel Dekker, Inc, New York (1986), Chap. 2.
12 U. Narusawa and G. S. Springer, *J. Colloid Interface Sci.*, **50**, 392 (1975).
13 K. J. Beverley, J. H. Clint, and P. D. I. Fletcher, *Phys. Chem. Chem. Phys.*, **1**, 149 (1999).
14 S. Lerdkanchnaporn and D. Dollimore, *Thermochim. Acta*, **324**, 15 (1998).
15 H. Hertz, *Ann. Phys.*, **17**, 177 (1882).
16 M. Knudsen, *Ann. Phys*, **47**, 697 (1915).
17 W. J. Moore, ''Physical Chemistry,'' Prentice-Hall, New Jersey (1962), Chap. 7.
18 R. Marek and J. Straub, *Int. J. Heat Mass Transfer*, **44**, 39 (2001).
19 J. M. Smith and H. C. Van Ness, ''Introduction to Chemical Engineering Thermodynamics,'' McGraw-Hill Kogakusha Ltd, Tokyo (1975).
20 R. M. Stephenson and S. Malamowski, ''Handbook of the Thermodynamics of Organic Compounds,'' Elsevier, New York (1987).
21 M. Ooki (editor-in-chief), ''Kagakubenran (Handbook of Chemistry),'' 4th ed, Maruzen Co., Tokyo (1993), Chap. 8, p. II-130.
22 J. J. Jasper, *J. Phys. Chem. Ref. Data*, **1**, 841 (1972).
23 T. K. Xia and U. Landman, *J. Chem. Phys.*, **101**, 2498 (1994).